

Zr Alloy Corrosion and HPU Mechanisms, Vol. III

Authors

Clément Lemaignan
Voreppe, France

Reviewed by

Audrius Jasiulevicius
Märsta, Sweden



A.N.T. INTERNATIONAL®

© January 2021

Advanced Nuclear Technology International
Spinnerivägen 1, Mellersta Fabriken plan 4,
448 50 Tollerød, Sweden

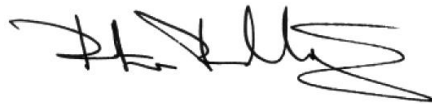
info@antinternational.com

www.antinternational.com

Disclaimer

The information presented in this report has been compiled and analysed by Advanced Nuclear Technology International Europe AB (ANT International®) and its subcontractors. ANT International has exercised due diligence in this work, but does not warrant the accuracy or completeness of the information. ANT International does not assume any responsibility for any consequences as a result of the use of the information for any party, except a warranty for reasonable technical skill, which is limited to the amount paid for this report.

Quality-checked and authorized by:

A handwritten signature in black ink, appearing to read 'Peter Rudling', written in a cursive style.

Mr Peter Rudling, President of ANT International

Contents

1	Physics of Zr alloy oxidation mechanisms	1-1
1.1	Overview of the corrosion mechanisms	1-1
1.2	Microstructure and oxide phases	1-5
1.2.1	The zirconium oxide ZrO ₂	1-5
1.2.2	The growth of the oxide on the metallic alloy	1-9
1.2.3	Undulation of the M/O interface	1-12
1.2.4	Stress in the oxide	1-13
1.2.4.1	Measurements of the stresses	1-13
1.2.4.2	Stress distribution and impact	1-15
1.2.5	Second phases in the oxide	1-17
1.2.6	Oxidation kinetic transition	1-20
1.2.6.1	Temperature distribution and impact	1-22
1.2.6.2	Effects of environmental chemistry	1-22
1.2.6.3	Nodular corrosion	1-23
1.2.6.4	Effects of irradiation	1-25
1.2.6.5	Irradiation damage in zirconia	1-27
1.2.6.6	Irradiation damage in the Zr alloys	1-30
1.2.6.7	Impact of irradiation on corrosion	1-32
2	Hydrogen Pick-Up	2-1

References

Nomenclature

List of Abbreviations

Unit conversion

1 Physics of Zr alloy oxidation mechanisms

With respect to the Zr alloy corrosion and HPU phenomena, numerous reviews have been issued since the early days of the nuclear industry and continue to be published e.g. [Cox et al., 1998] [Cox, 2005] [Allen et al., 2012] [Motta et al., 2015]. They provide updated examinations and explanations of the Zr alloy oxidation phenomena observed in reactors, in autoclaves or during analytical experiments. If the general contributions of most of the major parameters, and their interactions, are roughly understood, for the details of the mechanisms involved, we are far from a complete understanding. Consequently, these documents, and often most of the publications of the subject of Zr alloy corrosion and hydrogen pick-up (HPU), are scattered with sentences such as "... but a complete understanding of ... is still lacking.", "The question of whether ... is yet to be resolved." or "...has yet to be elucidated...".

Thus the following pages will limit themselves to an introduction to the best understood mechanisms of Zr alloys corrosion and HPU mechanisms, with the aim of giving a "mental image of the phenomena", more than discussing in detail all the controversial aspects of the current scientific debates. We hope that this will help the reader to have a fair feeling of what is important in the understanding of these phenomena. However various comments will be given on the degree of confidence that should be given to a selection of specific observations, in order help the reader also to have a critical perception of any new contributions he could have to analyse, in connection with the information provided by fuel vendors.

1.1 Overview of the corrosion mechanisms

Zr has high affinity for oxygen and, in contact with oxygen, will either dissolve oxygen or form compounds (oxides and sub-oxides). The thermodynamic equilibrium of zirconium in contact with oxygen is an oxide, the zirconia (ZrO_2), with a very high standard formation enthalpy ΔG (ZrO_2) of $1402 \text{ kJ}\cdot\text{mol}^{-1}$ (reduced to $965 \text{ kJ}\cdot\text{mol}^{-1}$ at $360 \text{ }^\circ\text{C}$). Zr is therefore a very strong reducing element and is expected to oxidise in almost any oxygen-bearing environment. Fortunately, the oxide forming on the surface of Zr has a protective character and Zr is practically not oxidising at room temperature. At higher temperatures, corresponding to nuclear reactor operating conditions, slow diffusion of oxygen in the zirconia is possible and Zr and its alloys develop oxide layers at low rates. The aim of this chapter is to give a general overview of the physics of the mechanisms involved in Zr alloy oxidation, in order to better understand the origins of the behaviour observed in power reactors, that are described in detail in Section 4 in Corrosion and Hydrogen Pickup Behaviour of Zr Alloys, Volume I [Rudling et al., 2018] and Corrosion and Hydrogen Pickup Behaviour of Zr Alloys, Volume II [Garzarolli and Rudling, 2020].

Once a thin oxide layer starts to form in high temperature water or steam ($250 - 500 \text{ }^\circ\text{C}$), it acts as a diffusion barrier of the species and the oxide growth rate is reduced as the layer thickens, leading to a parabolic corrosion rate, according to the classical Wagner oxidation theory [Wagner, 1933]. The oxide thickness in water follows then, at least at the beginning, a simple evolution rate with time:

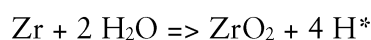
Equation 1-1:
$$\varepsilon = C * t^n$$

where ε is the oxide thickness, C a kinetic constant, t the time and n the exponent, whose value generally ranges between 0.3 and 0.5. The thickness of the oxide layer is measured either by weight gain, by non-destructive examination (NDE) techniques on irradiated fuel rods or destructively by metallography after corrosion tests. The equivalence between weight gain and oxide thickness gives that $15 \text{ mg}\cdot\text{dm}^{-2}$ corresponds approximately to $\sim 1 \text{ }\mu\text{m}$ of oxide. The kinetic constant includes all the rate-controlling mechanisms, especially the diffusion coefficients of the species. In the case of O in ZrO_2 , the diffusion is a thermo-activated process, with an activation energy roughly equal to $100 \text{ kJ}\cdot\text{mol}^{-1}$.

The rate controlling mechanism at this step of the corrosion is the diffusion of ions, counterbalanced by a flow of electrons in the oxide layer. In the case of Zr alloys, the diffusion rate of the oxygen ions in the zirconia is very fast, compared to the diffusion rate of the cation Zr^{4+} . The impact of this very high difference in mobilities is that the interaction of Zr with O occurs at the metal-oxide (M/O)

2 Hydrogen Pick-Up

During the reaction of Zr with water in the corrosion process, an important by-product is the hydrogen. The combined reactions at the anodic and cathodic sites can be expressed as the Equation 1-5:



The hydrogen released by the cathodic reaction (Equation 1-2) is a matter of concern in the case of the Zr alloys. One could expect that the atomic, unbound hydrogen atoms could recombine between themselves and form a hydrogen molecule that would dissolve in water. This is the most frequent mechanism occurring during oxidation in water for most other metals. However in the case of Zr and Zr alloys (as well as for Ti and Hf alloys), a significant fraction of the H released by the dissociation of water is migrating into the metal, where it forms a solid solution or, above the solubility limit, precipitates as hydrides.

Would the high hydrogen content in the metal not be detrimental for the mechanical properties of the alloys, this phenomenon would have remained a scientific curiosity. Unfortunately, the embrittlement induced by a high hydride volume fraction alters the capability of the hydrated components to support loadings and plastic strains, impacting their safety behaviour. The physics and the mechanisms of hydrogen pick-up (HPU) are therefore of uppermost importance and should be examined in detail. HPU remains a matter of high concern, but unfortunately the mechanisms of HPU are poorly understood and remain matter of controversy, while the phenomenon remains highly undesired.

A striking point with respect to the HPU is that the nascent hydrogen atoms are not supposed to dissolve in the metal, but should form H₂ molecules and dissolve in the coolant. The thermodynamics of H and its compounds states that, starting from isolated H atoms, the free energy release for the recombination of two nascent H* atoms to form a H₂ molecule dissolved in water is higher than for the dissolution of these atoms in the metal as a Zr(H) solid solution. Thus, the HPU phenomenon is not driven by the thermodynamics, but by coupled flows of O and H, the oxygen ions dragging the hydrogen atoms in their migration to the M/O interface.

Two major points were observed early in the history of HPU investigations:

- The hydrogen that is picked-up by the metal is not the H₂ dissolved in the coolant, but the H atoms released by the reaction of water at the W/O interface. The fact that HPU is independent of the amount of H₂ dissolved in the coolant, even at very concentrations, supports also this conclusion. It has also been confirmed by corrosion experiments with water in which gaseous tritium (³H₂) has been dissolved [Cox et al., 1998]. The Zr alloy remained free of tritium. Only the hydrogen (¹H) from the dissociated water molecules was migrating to the M/O interface, to dissolve in the metal.
- A very large difference in HPU between Zry2 and Zry4 was observed early, the later showing a much lower HPU fraction. A systematic examination of the impact of the transition metal additions (forming SPP's) allowed focusing on the nickel as a catalyst for the ingress of H in the metal [Cox, 1976]. This led to the choice of Zry-4 composition, where the Ni replaced by small increases in Fe and Cr.

Two main mechanisms of H migration must be considered: Bulk diffusion through the zirconia and bypass via intermetallic unoxidised precipitates.

The diffusion of hydrogen through the zirconia layer is known to be very limited. The diffusion coefficients of H in ZrO₂ have been measured and a large scatter exists among the reported values [Cox & Pemsler, 1968] [Khatamian, 1997]. The orders of magnitude of the different experiments still agree, with typical values of $D_{\text{H}/\text{ZrO}_2} \sim 10^{-19} \text{ to } 10^{-20} \text{ m}^2 \text{ s}^{-1}$ at 350 °C. With such low diffusion coefficients, significant transport of hydrogen through a pure zirconia layer cannot be considered, except for oxide thickness smaller than 0.1 μm, not relevant for our concern.

This restriction can be overcome by the consideration of the dopants present in the zirconia layers grown on alloys. Recent advanced analytical experiments show that the zirconia layers are far from

References

- Adamson, R. B., Coleman, C. E., Griffiths, M., *Irradiation creep and growth of zirconium alloys: A critical review*. J Nucl Mater, 521, pp. 167–244, 2019.
- Adamson, R., Lutz, D., and Davies, J., *Hot Cell Observations of Shadow Corrosion Phenomena*, Proceedings Fachtagung der KTG-Fachgruppe, Brennelemente und Kernbautelle, Forschungszentrum, Karlsruhe, Feb. 29–Mar. 1, 2000.
- Allen, T. R., Konings, R. J. M., Motta, A. T., *Corrosion of Zirconium Alloys*. In *Comprehensive Nuclear Materials* (1st ed., Vol. 5). Elsevier Inc., 2012.
- Andrieu, C., Ravel, S., Ducros, G., Lemaignan, C., *Release of fission tritium through Zircaloy-4 fuel cladding tubes*. Journal of Nuclear Materials, 347, pp. 12–19, 2005.
- Averin, S. A., Panchenko, V. L., Kozlov, A. V., Sinelnikov, L. P., Shishov, V. N., Nikulina, A., *Evolution of dislocation and precipitate structure in Zr alloys under long-term irradiation*. ASTM-STP, 1354, pp. 105–121, 2000.
- Bai, X. M., Zhang, Y., Tonks, M. R., *Strain effects on oxygen transport in tetragonal zirconium dioxide*. Physical Chemistry Chemical Physics, 15, pp. 19438–19449, 2013.
- Bouvier, Pierre, Djurado, E., Lucazeau, G., Bihan, T., *High-Pressure Structural Evolution of Undoped Tetragonal Nanocrystalline Zirconia*. Physical Review B, 62, pp. 8731–8737, 2000.
- Bouvier, P., Godlewski, J., Lucazeau, G., *A Raman study of the nanocrystallite size effect on the pressure-temperature phase diagram of zirconia grown by zirconium-based alloys oxidation*. Journal of Nuclear Materials, 300, pp. 118–126, 2002.
- Brossmann, U., Würschum, R., Södervall, U., Schaefer, H. E., *Oxygen diffusion in ultrafine grained monoclinic ZrO₂*. Journal of Applied Physics, 85, pp. 7646–7654, 1999.
- Burns, W. G., Moore, P. B., *Water radiolysis and its effect upon in-reactor Zircaloy corrosion*. Radiation Effects and Defects in Solids, 30, pp. 233–242, 1976.
- Buttin, P., Malki, B., Barberis, P., Baroux, B., *Numerical analysis of the galvanic coupling in the shadow corrosion of zirconium alloy*. Journal of Nuclear Materials, 420, pp. 591–596, 2012.
- Buxton, G V, Elliot, A. J., *High temperature water radiolysis and its relevance to reactor coolant*. Proc. JAIF Intl. Conf. Water Chem. Nucl. Power Plants, Fukui City, Japan, pp. 283–288, 1991.
- Buxton, George V, Mulazzani, Q. G., Ross, A. B., *Critical Review of Rate Constants for Reactions of Transients from Metal Ions and Metal Complexes in Aqueous Solution*. Journal of Physical and Chemical Reference Data, 24, pp. 1055–1349, 1995.
- Chan, S. -K, Fang, Y., Grimsditch, M., Li, Z., Nevitt, M. V., Robertson, W. M., Zouboulis, E. S., *Temperature Dependence of the Elastic Moduli of Monoclinic Zirconia*. Journal of the American Ceramic Society, 74, pp. 1742–1744, 1991.
- Charquet, D., Hahn, R., Ortlieb, E., Gros, J. P., Wadier, J. F., *Solubility limits and formation of intermetallic precipitates in Zr Sn Fe Cr alloys*. ASTM-STP, 1023, pp. 405–422, 1989.
- Chen, X., Bai, X. D., Deng, P., Peng, D., Liu, X., Xiyou, J., Cailiao, G., *Potential-pH diagrams of Zr-H₂O system at the increased temperatures*. Rare Metal Materials and Engineering, 33, pp. 710–713, 2004.
- Cheng, B. and Adamson, R. B., *Mechanistic Studies of Zircaloy Nodular Corrosion*, ASTM STP 939, 7th Inter^{natl.} Conf. on Zirconium in the Nuclear Industry, Strasbourg, France, June 24–27, 1985.

Nomenclature

t	Time
C, K	Various coefficients (defined locally in the text)
D_B	Grain boundary diffusion coefficient
D_V	Bulk diffusion coefficient
E	Modulus of Elasticity (Young's modulus)
R	γ irradiation intensity
E_{elast}	Stored elastic energy
α	Thermal expansion coefficient
ε	Oxide thickness
γ_s	Surface Energy
σ	Stresses
σ_e	Electronic conductivity
ΔG	Standard formation enthalpy
ΔT	Temperature change

List of Abbreviations

APT	Atom Probe Tomography
BWR	Boiling Water Reactor
CSZ	Ca Stabilised Zirconia
dpa	Displacement per atom
EIS	Electrochemical Impedance Spectroscopy
FIB	Focussed Ion Beam
G	Radiolytic species formation rate
GB	Grain Boundary
HPU	Hydrogen Pick Up
HPUF	HPU fraction
LHGR	Linear Heat Generation Rate
M/O	Metal / Oxide (interface)
MTR	Material Testing Reactors
NDE	Non-Destructive Examination
PB	Pilling-Bedworth ratio
PD	Point Defect
PWR	Pressurised Water Reactor
RIC	Radiation Induced Conductivity
RIED	Radiation Induced Electrical Degradation
S/V	Surface to Volume (ratio)
RT	Room Temperature
SEM	Scanning Electron Microscope
SIMS	Secondary Ion Mass Spectroscopy
SPP	Second Phase Particles (or Precipitates)
TEM	Transmission Electron Microscope
TM	Transition Metal
W/O	Water / Oxide (interface)
YSZ	Y Stabilised Zirconia

Unit conversion

TEMPERATURE		
$^{\circ}\text{C} + 273.15 = \text{K}$	$^{\circ}\text{C} \times 1.8 + 32 = ^{\circ}\text{F}$	
T(K)	T($^{\circ}\text{C}$)	T($^{\circ}\text{F}$)
273	0	32
289	16	61
298	25	77
373	100	212
473	200	392
573	300	572
633	360	680
673	400	752
773	500	932
783	510	950
793	520	968
823	550	1022
833	560	1040
873	600	1112
878	605	1121
893	620	1148
923	650	1202
973	700	1292
1023	750	1382
1053	780	1436
1073	800	1472
1136	863	1585
1143	870	1598
1173	900	1652
1273	1000	1832
1343	1070	1958
1478	1204	2200

Radioactivity	
1 Sv	= 100 Rem
1 Ci	= 3.7×10^{10} Bq = 37 GBq
1 Bq	= 1 s^{-1}

MASS	
kg	lbs
0.454	1
1	2.20

DISTANCE	
x (μm)	x (mils)
0.6	0.02
1	0.04
5	0.20
10	0.39
20	0.79
25	0.98
25.4	1.00
100	3.94

PRESSURE		
bar	MPa	psi
1	0.1	14
10	1	142
70	7	995
70.4	7.04	1000
100	10	1421
130	13	1847
155	15.5	2203
704	70.4	10000
1000	100	14211

STRESS INTENSITY FACTOR	
MPa $\sqrt{\text{m}}$	ksi $\sqrt{\text{inch}}$
0.91	1
1	1.10